Development 133, 3317-3328 (2006) doi:10.1242/dev.02494

# An unusual Zn-finger/FH2 domain protein controls a left/right asymmetric neuronal fate decision in *C. elegans*

**Robert J. Johnston, Jr[1], John W. Copeland[2], Marc Fasnacht[1,3], John F. Etchberger[1], Jun Liu[4], Barry Honig[1,3] and Oliver Hobert[1,*]**

Gene regulatory networks that control the terminally differentiated state of a cell are, by and large, only superficially understood. In a mutant screen aimed at identifying regulators of gene batteries that define the differentiated state of two left/right asymmetric *C. elegans* gustatory neurons, ASEL and ASER, we have isolated a mutant, *fozi-1*, with a novel mixed-fate phenotype, characterized by de-repression of ASEL fate in ASER. *fozi-1* codes for a protein that functions in the nucleus of ASER to inhibit the expression of the LIM homeobox gene *lim-6*, neuropeptide-encoding genes and putative chemoreceptors of the GCY gene family. The FOZI-1 protein displays a highly unusual domain architecture, that combines two functionally essential C2H2 zinc-finger domains, which are probably involved in transcriptional regulation, with a formin homology 2 (FH2) domain, normally found only in cytosolic regulators of the actin cytoskeleton. We demonstrate that the FH2 domain of FOZI-1 has lost its actin polymerization function but maintains its phylogenetically ancient ability to homodimerize. *fozi-1* genetically interacts with several transcription factors and micro RNAs in the context of specific regulatory network motifs. These network motifs endow the system with properties that provide insights into how cells adopt their stable terminally differentiated states.

**KEY WORDS: *Caenorhabditis elegans*, Left/right asymmetry, Neuronal cell fate, Zn-finger transcription factor, FH2 domain**

## INTRODUCTION

The differentiated state of a cell is defined by the array of genes (‘gene battery’) expressed by that cell (Davidson, 2001). The mechanisms controlling the gene expression profile of a single cell are sometimes surprisingly complex. Feedback, feed-forward and multi-tier parallel pathways are required to attain, stabilize and maintain the complete signature of a cell-specific program of gene expression. Though these types of regulatory networks have been rigorously described in single cell organisms (e.g. Lee et al., 2002; Shen-Orr et al., 2002), a thorough analysis of complex regulatory networks in multicellular organisms has only been described in few isolated examples (Davidson, 2001). In complex metazoan organisms, the functional analysis of gene regulatory networks are often complicated by various factors, including the pleiotropies caused by mutations in regulatory genes and the unavailability of a sufficient number of molecular markers that define cellular fates on a single cell level.

To address the mechanisms controlling single cell-specific gene expression programs, we have characterized the neuronal subclass diversification process executed by the ASE class of gustatory neurons in *C. elegans*. This neuron class consists of a pair of two bilaterally symmetric neurons, ASE left (ASEL) and ASE right (ASER) (Fig. 1A). ASEL is the primary sodium sensor, whereas ASER is the primary $Cl^-$ and $K^+$ sensor (Pierce-Shimomura et al., 2001). The left/right asymmetric (‘lateral’) separation of chemosensory capacities endows the worms with the ability to discriminate between distinct chemosensory cues and thereby widens its chemosensory repertoire. Other than these functional differences, the ASE pair of neurons are bilaterally symmetric by anatomical criteria such as cell body position, axodendritic structure and synaptic connectivity (White et al., 1986).

ASEL and ASER subclass diversification is defined by an array of left/right asymmetrically expressed cell fate markers including specific subsets of guanylyl cyclase receptors, encoded by GCY genes, and FMRFamide-type neuropeptides, encoded by FLP genes, (Fig. 1A) (Johnston et al., 2005; Ortiz et al., 2006; Yu et al., 1997). We have previously shown that a network of micro RNAs (miRNAs) and transcription factors controls ASEL/R cell fate diversification (Fig. 1A) (Chang et al., 2004; Chang et al., 2003; Hobert et al., 1999; Johnston and Hobert, 2003; Johnston et al., 2005; Johnston and Hobert, 2005). A bi-stable feedback loop constituted by these regulatory factors is an essential network motif required for the establishment and stabilization of lateral ASE fate. In this loop, ASEL-specific inducer genes, such as the *lsy-6* miRNA and *die-1* transcription factor, activate expression of other ASEL-specific inducer and effector genes and repress ASER-specific inducer and terminal genes. By contrast, ASER-specific inducer genes such as the *mir-273* miRNA and *cog-1* transcription factor control expression of ASER-specific genes and repression of ASEL-specific genes. Genetic experiments indicate that *lsy-6* and its upstream activator, the Zn-finger transcription factor *lsy-2*, provides the input into the loop, whereas the output of the loop is provided by the Zn-finger transcription factor *die-1* (Johnston et al., 2005; Johnston and Hobert, 2005) (Fig. 1A).

In this paper, we describe the cloning and characterization of *fozi-1*, a novel protein containing two Zn fingers and a single FH2 domain. This gene plays a role downstream of the bi-stable feedback loop to repress expression of ASEL-specific effector genes in ASER. We anticipate that the complex regulatory network described here will provide a paradigm for subtype fate specification in other cellular contexts.

[1]Howard Hughes Medical Institute, Department of Biochemistry and Molecular Biophysics, Columbia University Medical Center, 701 W. 168th Street, New York, NY 10032, USA. [2]Department of Cellular and Molecular Medicine, University of Ottawa, Ottawa, Ontario K1H 8M5, Canada. [3]Howard Hughes Medical Institute, Department of Biochemistry and Molecular Biophysics, Center for Computational Biology and Bioinformatics, Columbia University Medical Center, 1130 St Nicholas Avenue, Room 815, New York, NY 10032, USA. [4]Department of Molecular Biology and Genetics, Cornell University, Ithaca, NY 14853, USA.

*Author for correspondence (e-mail: or38@columbia.edu)

**Accepted 13 June 2006**

## MATERIALS AND METHODS

### Strains, DNA and transgenes

Strains used for mapping, RNAi sensitization and manipulation of ASE development, as well as transgenes used to assess or manipulate ASE fate have all been previously described (Chang et al., 2004; Chang et al., 2003; Hobert et al., 1999; Hodgkin and Doniach, 1997; Johnston and Hobert, 2003; Johnston et al., 2005; Simmer et al., 2002).

### List of new transgenes

All contain the *elt-2::gfp* (Fukushige et al., 1998) as injection marker and are named as follows: *otEx2179-2182*, *Ex[fozi-1 genomic; elt-2::gfp]*; *otEx2190-2193*, *Ex[fozi-1::gfp; elt-2::gfp]*; *otEx2512-2515*, *Ex[gcy-5$^{prom}$::fozi-1cDNA::gfp; elt-2::gfp]*; *otEx2523-2526*, *Ex[gcy-5$^{prom}$::fozi-1cDNAΔZn-finger::gfp; elt-2::gfp]*; *otEx2516, 2518, 2520*, *Ex[gcy-5$^{prom}$::fozi-1cDNAΔFH2::gfp; elt-2::gfp]*; and *otEx2534*, *Ex[ceh-36$^{prom}$::fozi-1cDNA::gfp; elt-2::gfp]*.

### DNA for transgenic lines

The genomic *fozi-1* locus was amplified from N2 genomic DNA using the primers 5′-CACCCCAAGATGGTAGTAATCC and 5′-GAAGAACTGGACAATTCGG.

#### *fozi-1::gfp*

*fozi-1::gfp* was generated by PCR fusion (Hobert, 2002). The first PCRs were carried out on genomic DNA with 5′-GGAGTGGACGATGACATTGTG and 5′-AGTCGACCTGCAGGCATGCAAGCTAGGAGACGAGACATTGATGTG and on the *gfp* sequence in pP95.75 with 5′-CACATCAATGTCTCGTCTCCTAGCTTGCATGCCTGCAGGTCGACT and primer D (Hobert, 2002). The fusion PCR was carried out with the non-nested primer 5′-GGAGTGGACGATGACATTGTG and primer D* (Hobert, 2002).

#### *gcy-5$^{prom}$::fozi-1cDNA::gfp and ceh-36$^{prom}$::fozi-1cDNA::gfp*

The *fozi-1*-coding sequence from start to stop codon was PCR amplified from the EST clone yk288g3 with the primers 5′-TTGGATCCATGATGCTTGCATCATCAGCG and 5′-AATGGCCAAGGAGACGAGACATTGATGTG. The amplicon was cloned into *gcy-5$^{prom}$::gfp* and *ceh-36$^{prom}$::gfp* vector constructs that will be described elsewhere in detail.

#### *gcy-5$^{prom}$::fozi-1cDNAΔZn-finger::gfp*

The construct *gcy-5$^{prom}$::fozi-1cDNA::gfp* was mutated by standard mutagenesis using the primers 5′-CTATCCCTGTACATTTCAATATgGATTAGCGGGTGACCCGATCAG and 5′-CTGATCGGGTCACCCGCTAATCcATATTGAAATGTACAGGGATAG.

#### *gcy-5$^{prom}$::fozi-1cDNAΔFH2::gfp*

Truncated *fozi-1* was amplified from the *fozi-1* EST clone yk288g3 using the primers 5′-ttggatccATGATGCTTGCATCATCAGCG and 5′-aatggccaAATTGGCTGAATCGGAATTATAGATGATGACAAGG. The resulting amplicon was subcloned into the *gcy-5$^{prom}$::gfp* vector construct.

### Genetics

The genetic screen from which *ot61* was isolated has been described before (Johnston et al., 2005). Briefly, animals carrying the *otIs3* transgene, which express *gcy-7$^{prom}$::gfp* exclusively in ASEL, were mutagenized with EMS. F1 progeny were singled and F2 progeny were scored under a Zeiss SV6 fluorescent dissecting microscope. Mutant mapping was carried out using a combination of single nucleotide polymorphisms from the Hawaiian wild-type isolate CB4856 (Hodgkin and Doniach, 1997) and three-factor mapping with the visible markers *dpy-17* and *unc-49*.

### Biochemical analysis of the FOZI-1 FH2 domain

The cDNA encoding the FOZI-1 FH2 domain (residues 367-733) was subcloned by standard techniques into pGEX-6P2 and expressed as a GST fusion protein in *E. coli* strain BL21. FH2$^{FOZI-1}$ protein was purified by cleavage from the GST moiety (Copeland et al., 2004). Protein purity was assessed by Coomassie Blue staining of samples subjected to SDS-PAGE, concentration was determined by Bradford and by OD280. The isolated FH2 domain (0.4 μM) was added to G-actin (4 μM, 5% pyrene-actin) for in vitro actin polymerization assays (Cytoskeleton) according to the supplied protocol. For cross-linking, the purified FH2$^{FOZI-1}$ domain (20 nM) was incubated at room temperature for 60 minutes in HEK buffer with 30 μM of the crosslinker *Bis*-maleimidohexane (Pierce) dissolved in DMSO or DMSO alone. A second control sample was boiled for 10 minutes in 2% SDS prior to crosslinking. The crosslinking reactions were quenched with 45 mM DTT and then subjected to SDS-PAGE. The proteins were transferred to PVDF membranes and visualized by immunoblotting with an anti-6xHis monoclonal antibody (Clontech).

## RESULTS

### Isolation of a novel ASE cell fate mutant

In order to identify genes essential for the ASEL/R cell fate decision, we performed screens for mutants defective in expression of the ASEL-specific *gcy-7$^{prom}$::gfp* reporter gene. We have previously termed mutants that arose from these screening efforts '*lsy*' mutants [for 'laterally symmetric' (Johnston and Hobert, 2003)]. The *lsy* mutants retrieved from past genetic screens fall into three phenotypic categories.

(1) Class I ('two ASEL') mutants. The ASER neuron loses expression of ASER-specific genes and gains expression of the normally ASEL-specific gene expression profile (examples: *cog-1, unc-37* mutants) (Chang et al., 2003).

(2) Class II ('two ASER') mutants. The ASEL neuron loses the ASEL-specific gene expression profile and displays the normally ASER-specific gene expression profile (examples: *lsy-6, die-1, lsy-2, ceh-36, lin-49* mutants) (Chang et al., 2004; Chang et al., 2003; Johnston and Hobert, 2003; Johnston and Hobert, 2005).

(3) Class III ('no ASEL/R') mutants. Complete loss of both asymmetric and symmetric features of the ASE neuron (example: *che-1* mutants) (Chang et al., 2003).

One recessive mutant allele identified in the screen, *ot61*, exhibits a unique phenotype not described previously. All *ot61* mutant animals display de-repression of *gcy-7$^{prom}$::gfp* in ASER (Fig. 1B). However, although the phenotype is completely penetrant (all animals show the defect), the levels of aberrant *gcy-7$^{prom}$::gfp* expression in ASER are variable. Sometimes, the level of aberrant *gcy-7$^{prom}$::gfp* expression in ASER is equivalent to the normal and unaffected *gcy-7$^{prom}$::gfp* expression in ASEL, but more often, the aberrant *gcy-7$^{prom}$::gfp* expression level in ASER is not as high as the *gcy-7$^{prom}$::gfp* expression level in ASEL (Fig. 1B, Table 1). The *fozi-1* mutant phenotype is therefore 'variably expressive'. This variable expressivity contrasts the previously described phenotype in the ASER neuron of class I ('two ASEL') mutant animals in which the level of aberrant *gcy-7$^{prom}$::gfp* expression in ASER always reaches levels indistinguishable from the level in ASEL (i.e. complete expressivity) (Chang et al., 2003). To determine whether this complete penetrance and partial expressivity applies to other ASEL-specific fate markers, we crossed *ot61* with animals containing the ASEL-specific *lim-6$^{prom}$::gfp* reporter transgene and again observed de-repression of the reporter gene with complete penetrance and variable expressivity (Fig. 1B).

### *fozi-1* encodes a protein with an unusual domain composition

Before characterizing the *ot61* phenotype in more detail, we first determined the molecular identity of the mutant locus. Given the variable expressivity of the *ot61* mutant phenotype, we were particularly interested in determining whether this phenotype is merely explained by a hypomorphic nature of the *ot61* allele. We mapped the *ot61* mutant to a small interval on chromosome III using a combination of SNP and three-factor physical mapping. Transformation rescue narrowed the position of the locus to a single

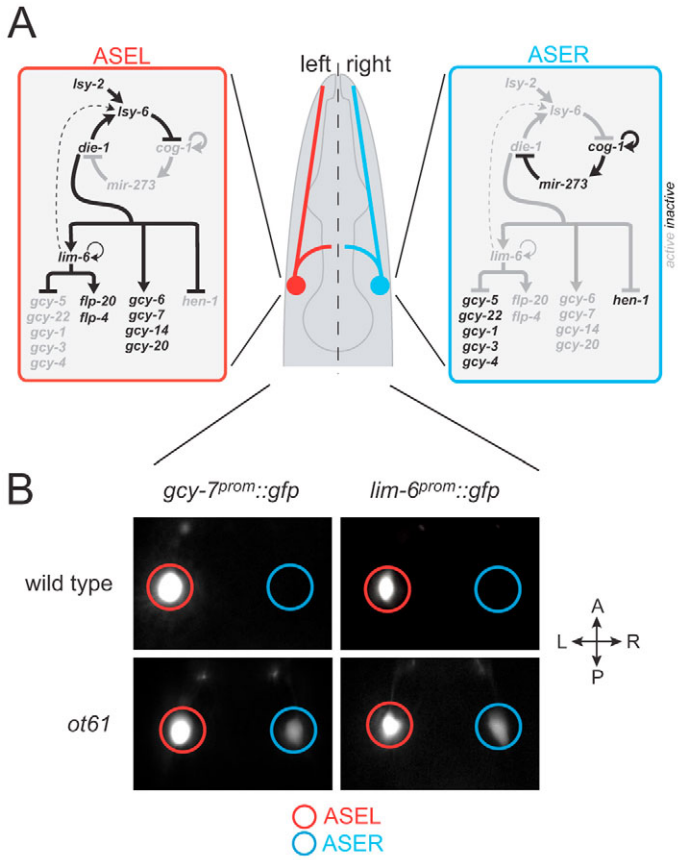


**Fig. 1. *fozi-1* mutants display a de-repression of ASEL-specific fate markers in ASER.** (**A**) Summary of previously described regulatory interactions that determine ASEL and ASER fate. Some permissively acting genes (Chang et al., 2003) are not shown for simplicity. (**B**) In *fozi-1(ot61)* mutants, ASEL-specific *gcy-7*$^{prom}$*::gfp* (*otIs3)* and *lim-6*$^{prom}$*::gfp (otIs114)* expression is de-repressed in ASER. See Table 1 and Fig. 4A for quantification.

cosmid, K01B6 (Fig. 2A), and RNA interference of a single predicted gene on that cosmid, *K01B6.1*, recapitulated the defects of *ot61* mutants (Table 1). We sequenced K01B6.1 in *ot61* mutant animals and found that it contains a nonsense mutation resulting in premature termination of the protein-coding sequence (Fig. 2B). Two additional alleles that delete essential parts of the predicted K01B6.1 gene phenocopy the *ot61* mutant allele (Fig. 2B; Table 1). Last, a genomic fragment that contains only the K01B6.1-coding sequences rescues the mutant phenotype (Fig. 3A). We conclude that the loss of *K01B6.1* function causes ASE differentiation defects.

The predicted *K01B6.1* gene structure was confirmed by analyzing an expressed sequence tag provided by Y. Kohara. The protein encoded by *K01B6.1* contains three readily recognizable motifs (Fig. 2B): (1) a Q-rich motif often found in transcription factors (Titz et al., 2006); (2) two C2H2 Zn fingers with a standard $CX_2CX_{11-13}HX_4H$ spacing normally found in DNA-binding transcription factors (Iuchi, 2001) (see Fig. S1 in the supplementary material); (3) a formin homology 2 (FH2) domain, which is surprising as this domain is normally found only in cytosolic actin-polymerizing proteins in which the domain catalyses actin polymerization (Zigmond, 2004). Owing to the unusual combination of the formin homology 2 and zinc-finger domains, we have named the gene *fozi-1* (pronounced 'fozzy-1').

*fozi-1* is highly conserved in all three available nematode genome sequences (see Fig. S1 in the supplementary material). No other predicted *C. elegans* protein contains a FH2 domain combined with C2H2 Zn fingers. Database searches revealed only a single non-nematode gene in the zebrafish *Danio rerio* genome sequence that is predicted to contain a FH2 domain combined with C2H2 Zn fingers (data not shown). However, as this gene is not confirmed by cDNA evidence, we cannot exclude the possibility of a genome assembly or gene prediction error.

## The ASER neuron adopts a 'mixed fate' in *fozi-1* mutants

After cloning *fozi-1*, two additional alleles of *fozi-1*, *cc607* and *tm563*, were made available to us. Like *ot61* mutants, *cc607* and *tm563* mutants are viable, fertile and display no obvious behavioral or morphological abnormalities. The *cc607* allele was retrieved from a screen for mesoderm lineage differentiation defects (J.L., unpublished). *cc607* is a putative molecular null allele as it encodes a nonsense mutation causing premature termination before both the Zn fingers and the FH2 domain (Fig. 2B). Using rescue assays, we show below that the Zn fingers are essential for *fozi-1* function. The other allele, *tm563*, kindly provided by a *C. elegans* knockout consortium, completely deletes the Q-rich domain-containing exon 3 and a large part of exon 4, including the first Zn finger and the first half of the second Zn finger (Fig. 2B). Owing to a premature stop codon introduced by the deletion, *tm563* can also be considered a molecular null allele. The availability of these two molecular null alleles allowed us to examine whether the variable phenotypic expressivity of *fozi-1(ot61)* mutants is merely a reflection of a partial loss of gene function. Crossing the putative null alleles *cc607* and *tm563* with the ASEL-specific *lim-6*$^{prom}$*::gfp* transgene, we observed gene expression defects essentially identical to those seen in *ot61* mutant animals (Table 1). At least in the context of the ASE subclass determination, *ot61* may therefore similarly be a null allele of *fozi-1*.

We examined the effect of the *fozi-1(cc607)*-null allele on several additional markers that define the ASEL fate, namely the two GCY genes *gcy-6* and *gcy-7* and the neuropeptide-encoding *flp-4* gene. We found that all examined ASEL fate markers are affected in a similar manner in that they become partly de-repressed in a completely penetrant manner (Fig. 4A). The incomplete and variably expressive de-repression of ASEL fate markers in the ASER neuron of *fozi-1*-null mutants suggests that additional, *fozi-1*-independent mechanism(s) must exist to prevent complete de-repression of the ASEL fate markers.

In contrast to all previously defined ASE cell fate mutants, the de-repression of ASEL terminal fate markers in the ASER neuron of *fozi-1* mutants is not accompanied by loss of ASER fate markers. Expression of the ASER-specific *gcy-4*, *gcy-5* and *hen-1* genes in *fozi-1* null mutants is indistinguishable from wild-type expression (Fig. 4B). Taken together, the ASEL neuron appears completely unaffected in *fozi-1* mutants in that ASEL markers are expressed and ASER fate markers are not de-repressed. By contrast, ASEL fate markers are de-repressed in ASER, but ASER fate markers remain unaffected. The ASER neuron therefore displays a novel 'mixed' phenotype in *fozi-1* mutants (Fig. 4C). Extending our previous mutant classification, we term this phenotype a 'class IV' phenotype.

## *fozi-1* acts in a left/right asymmetric manner in ASER, but not ASEL

The phenotypic analysis of *fozi-1* demonstrates that ASER, but not ASEL, is affected in *fozi-1* mutants. As *fozi-1* appears to encode a gene regulatory factor, the gene expression defects in ASER are

**Table 1. Phenotypic comparison of *fozi-1* alleles**

| *fozi-1* allele | Nature of allele | ASEL fate* ● ○ (L>0) | ● ◎ (L>R) | ● ● (L=R) | *n* |
|---|---|---|---|---|---|
| Wild type | – | 100% | 0% | 0% | >100 |
| RNAi† | Knockdown | 87% | 13% | 0% | 38 |
| *ot61* | Late nonsense | 0% | 82% | 18% | 116 |
| *cc607*‡ | Early nonsense | 0% | 84% | 16% | 115 |
| *tm563* | N-terminal deletion | 0% | 84% | 16% | 113 |

*Analyzed with the fate marker *lim-6$^{prom}$::gfp (otIs114).* Circles indicate *gfp* expression in ASEL (L) and ASER (R). White, no expression; gray, intermediate expression; black, wild-type expression.
†RNAi was performed in an *rrf-3* mutant background as previously described (Johnston and Hobert, 2005). Mock RNAi produced no phenotype (*n*>100).
‡The wild-type and *cc607* data are also shown in Fig. 4A.

most easily explained by *fozi-1* being expressed and acting in ASER. We tested this prediction by a variety of means, including gene expression pattern analysis, cell-specific rescue and mis-expression approaches.

In order to investigate *fozi-1* expression, we generated a construct, *fozi-1::gfp*, in which the genomic *fozi-1* locus is tagged with *gfp*. This construct efficiently rescues the *fozi-1* mutant phenotype (Fig. 3A). Transgenic, adult animals display *gfp* expression in the nucleus of the AWC and ASE neuron class (Fig. 3B and data not shown). No other expression was observed in head ganglia. Three out of four lines displayed a bias in expression to ASER; by contrast, expression in the AWCL/R neurons is bilaterally symmetric (Fig. 3B,C). To corroborate that *fozi-1* indeed functions in ASER, we generated a *gcy-5$^{prom}$::fozi-1 cDNA::gfp* construct in which the *gcy-5* promoter drives expression of *fozi-1* fused to *gfp* specifically in postmitotic ASER neurons. The *gfp* moiety confirmed that *fozi-1* was expressed and localized to the nucleus of transgenic animals. Four out of four *gcy-5$^{prom}$::fozi-1 cDNA::gfp* transgenic lines rescued the *lim-6$^{prom}$::gfp* de-repression defects in ASER observed in *fozi-1(cc607)*-null mutant animals. Taken together, expression and rescue experiments with the heterologous promoter demonstrate that *fozi-1* acts specifically in ASER to repress ASEL cell fate.

Transgenic lines that contain multiple copies of genomic *fozi-1* DNA show not only a rescue of the ASER defects of *fozi-1* mutants (Fig. 3A, right bar) but also show a partial repression of *lim-6* expression in ASEL (Fig. 3A, left bar). This ectopic activity of *fozi-1* correlates with the degree of ASEL versus ASER bias of *fozi-1::gfp* expression (Fig. 3C). Transgenic line 3, which shows the most bias to ASER rescues the ASER defect but has little impact on ASEL fate determination, while transgenic lines 1 and 4, which show a larger degree of *fozi-1::gfp* in both ASER and ASEL (Fig. 3C), show suppression of the ASEL fate marker *lim-6* in ASEL (Fig. 3A). These observations suggest that *fozi-1* may be sufficient to repress ASEL fate if overexpressed in ASEL. To corroborate this notion, we generated a *ceh-36$^{prom}$::fozi-1 cDNA::gfp* construct in which the *ceh-36* promoter drives equal expression of *gfp*-tagged *fozi-1* in both ASEL and ASER. Introduction of this construct into the *fozi-1(cc607)* mutant background showed equivalent repression of *lim-6$^{prom}$::gfp* expression in both ASEL and ASER (Fig. 3A). *fozi-1* is therefore sufficient to repress *lim-6* when ectopically expressed in ASEL. Taken together, we conclude that *fozi-1* expression is biased to ASER and that it acts autonomously to repress the expression of *lim-6* and other ASEL-specific genes in ASER.

Last, as two transcription factors in the ASEL/R cell fate regulatory network are repressed via 3′UTR dependent mechanisms (*cog-1*, *die-1*), we tested whether the 3′UTR of *fozi-1* contains cis-regulatory information that may contribute to the left/right asymmetric function of *fozi-1*. Using a sensor gene approach that revealed the 3′UTR-dependent regulation of the *cog-1* and *die-1* genes (Chang et al., 2004; Johnston and Hobert, 2003), we found this not to be the case (data not shown).

## Terminal differentiation genes are also controlled by pathways that act in parallel to *fozi-1* and *lim-6*

The results presented so far can be summarized as shown schematically in Fig. 4E. *fozi-1* is expressed in ASER and is required to repress ASEL-specific features in ASER. The incomplete nature of de-repression of the ASEL markers suggests one of two scenarios. In scenario 1, *fozi-1* acts together with an unknown repressor X to repress ASEL-specific features in ASER and only loss of both *fozi-1* and X causes complete de-repression of ASEL fate in ASER. Alternatively, in scenario 2, de-repression of ASEL markers in ASER of *fozi-1* is incomplete as an activator Y is missing in ASER (Fig. 4E).

The LIM homeobox gene *lim-6* is expressed in ASEL and its loss causes a mixed phenotype that is superficially the mirror image of the *fozi-1* loss-of-function phenotype. The ASER neuron is unaffected, but the ASEL neuron displays a ‘mixed phenotype’ characterized by a failure to repress ASER features in ASEL (Hobert et al., 1999; Johnston et al., 2005; Ortiz et al., 2006). Like in *fozi-1* mutants, the defects in *lim-6*-null mutants are also variably expressive (Fig. 4D), thereby suggesting the existence of *lim-6*-independent means to repress ASER fate (Fig. 4E). Consistent with the existence of a parallel pathway, repression of ASER fate markers induced by ectopic expression of the *lsy-6* miRNA in ASER does not absolutely require *lim-6* (Fig. 4D). We have previously shown that *lim-6* is also required to positively regulate the expression of ASEL-specific markers, namely the two FMRFamide-encoding genes *flp-4* and *flp-20* (Johnston et al., 2005). *lim-6*-null mutant animals show only a partially penetrant loss of *flp-4* and *flp-20* expression, again indicating the presence of a parallel pathway (indicated in by a factor Z in Fig. 4E). Taken together, these observations suggest that both *lim-6* and *fozi-1* require parallel pathways to exert their function in ASEL and ASER, respectively.

## *fozi-1* acts downstream of the bi-stable feedback loop

We tested how *fozi-1* gene function relates to the function of components of the bi-stable feedback loop that controls ASEL and ASER fate (Fig. 1A). We found that disruption of this bi-stable loop causes a ‘symmetrization’ of the normally left/right asymmetric expression of *fozi-1* (Fig. 5A). Specifically, in animals in which the ASEL-inducers *die-1* or the *lsy-6* miRNA are mutated, *fozi-1* expression becomes de-repressed in ASEL. In animals lacking the ASER-inducer *cog-1*, the bias of *fozi-1* expression to ASER is also lost. These results are consistent with our previous observations that the bi-stable feedback loop controls all features of the ASEL/R fate decision (Johnston et al., 2005).

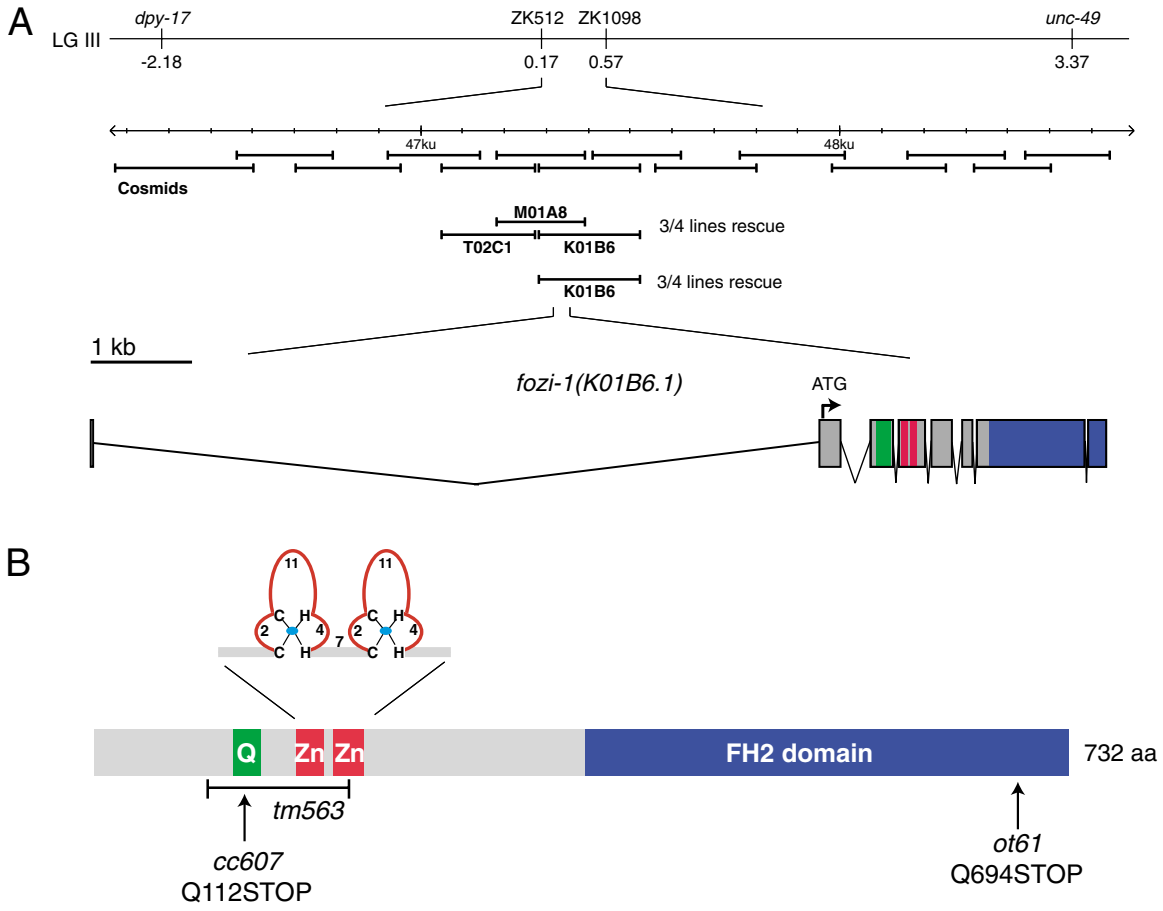


**Fig. 2. *fozi-1* encodes a protein with two Zn fingers and a formin homology 2 domain.** (**A**) Mapping of the *ot61* mutation. (**B**) Structure of the predicted FOZI-1 protein.

We corroborated the downstream role of *fozi-1* using two genetic epistasis tests. In animals in which the *lsy-6* miRNA is deleted, ASEL displays the complete ASER gene expression profile including the repression of *lim-6* expression (Johnston and Hobert, 2003). Repression of *lim-6* in *lsy-6(ot71)* null mutant animals requires *fozi-1* activity as *fozi-1(ot61); lsy-6(ot71)* double mutants display a de-repression of *lim-6$^{prom}$::gfp* in ASEL and ASER (Fig. 5B). The same genetic interaction is observed using *die-1* mutants. In *die-1(ot26)* mutant animals, *lim-6* expression is repressed in ASEL (Chang et al., 2004). This repression requires *fozi-1* as *die-1(ot26); fozi-1(ot61)* double mutants display a de-repression of *lim-6$^{prom}$::gfp* in ASEL and ASER (Fig. 5B). Together, these data demonstrate that *fozi-1* acts downstream of *die-1*, the output regulator of the bi-stable feedback loop (Fig. 5C).

In contrast to the partially expressive effects of *fozi-1* on *lim-6* expression, the effects of disruption of bi-stable loop components such as *die-1* or *cog-1* on *lim-6* expression are completely expressive. For example, levels of aberrant *lim-6* expression in ASER in *cog-1* mutants are similar to normal levels of *lim-6* expression in ASEL (Chang et al., 2003). The *fozi-1* parallel pathway that we evoked above (Fig. 4E), therefore, depends genetically on the activity of the bi-stable loop whose output regulator is the *die-1* gene. The most parsimonious way to present these regulatory interactions is shown in Fig. 5C with an arrow from *die-1* to *lim-6* that is parallel to the *fozi-1*-mediated regulation of *lim-6*. In other words, *lim-6* expression genetically requires both the presence of *die-1* and the absence of *fozi-1*.

Loss of *die-1* also causes a completely expressive de-repression of ASER fate in ASEL (Chang et al., 2004), which contrasts the partially expressive de-repression of ASER fate in the ASEL neuron of *lim-6*-null mutants. The *lim-6*-parallel pathway that we evoked above (Fig. 4E), therefore also depends on the loop output regulator *die-1*. The most parsimonious explanation of the genetic interactions is that the factor that acts in parallel to *lim-6* (factor Z in Fig. 4E) is *die-1* itself (Fig. 5C).

A loss of the *lim-6* LIM homeobox gene, which acts downstream of the bi-stable feedback loop (Fig. 1A) causes a partially penetrant defect in maintaining the left/right asymmetric expression of loop components (Johnston et al., 2005) (broken line in Fig. 1A). As *lim-6* is de-repressed in ASER of *fozi-1* mutants, we asked whether a similar partially penetrant defect can be observed in *fozi-1* mutants, and we indeed find this to be the case (Fig. 5D,E). Moreover, as would be expected from a partial disruption of activity of bi-stable loop components in *lim-6*-null mutants, asymmetric *fozi-1* expression is also partially affected in *lim-6* mutants (Fig. 5A).

Taken together, left/right asymmetric *fozi-1* expression is controlled by components of the bi-stable feedback loop and asymmetric *fozi-1* augments the maintenance of the asymmetric expression of loop components, probably through the regulation of *lim-6* expression.

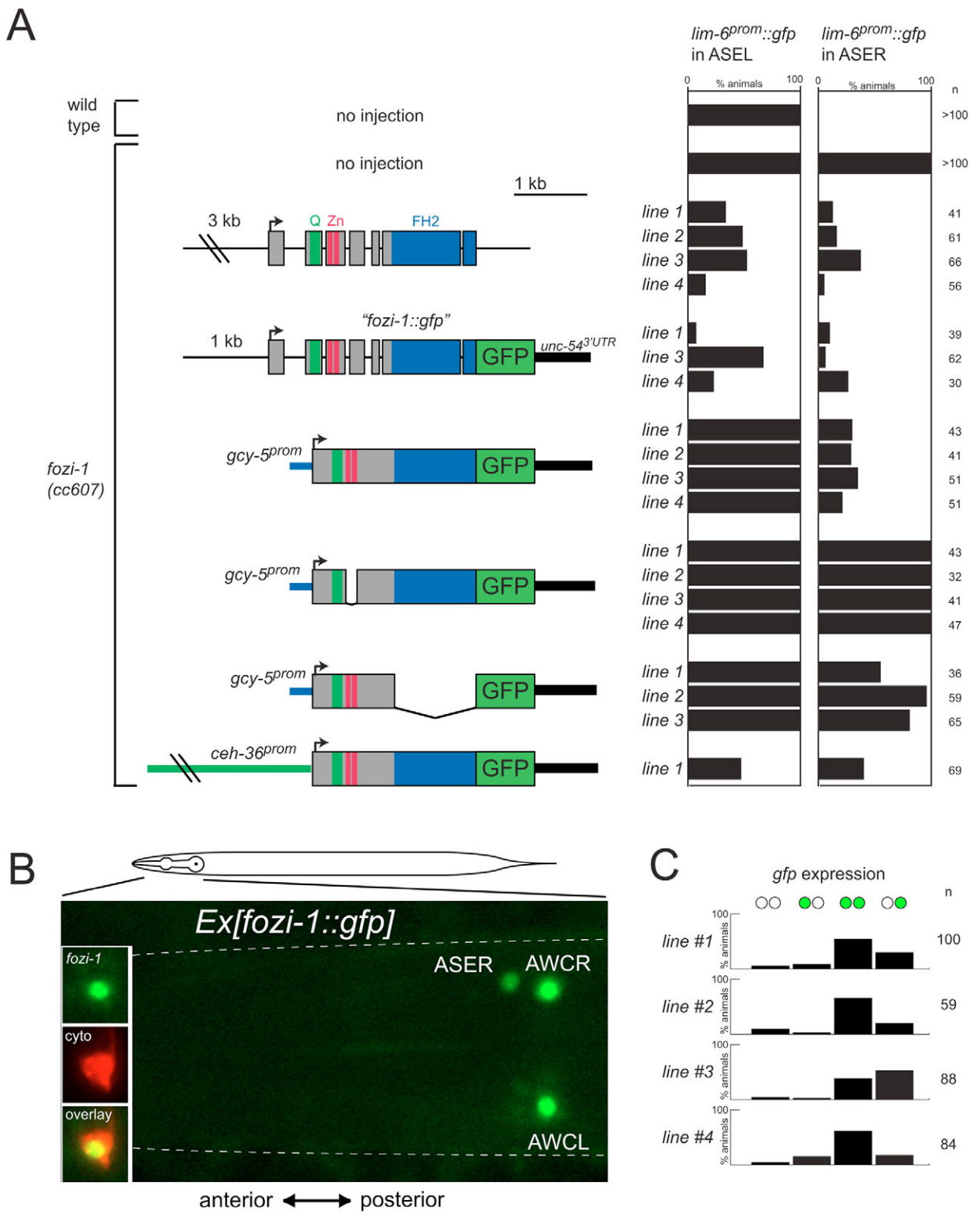


**Fig. 3. Rescue, expression, site of action and domain requirements of *fozi-1*.** (**A**) Rescue of the *fozi-1* mutant phenotype. The constructs do not contain the first, non-coding exon of the *fozi-1* gene, which is located >7 kb upstream of the ATG-containing second exon (Fig. 2A). The right column indicates rescue of the *fozi-1* defect, i.e. suppression of aberrant *lim-6* expression in ASER, and the left column indicates suppression of normal *lim-6* expression in ASEL fate, caused by ectopic expression of *fozi-1*. All constructs show similar expression levels and exclusive localization to the nucleus. (**B**) A representative *fozi-1::gfp*-expressing animal, showing *gfp* expression in ASER but not ASEL, and in the two olfactory neurons AWCL and AWCR. Broken lines approximately indicate the head of the worm. The insets show that *fozi-1::gfp* predominantly localizes to the nucleus. The red 'cyto' marker is dsRed2 protein, expressed under control of the *ceh-36* promoter (*otIs151* transgene). (**C**) Three out of four *fozi-1::gfp*-expressing transgenic, wild-type lines display varying levels of asymmetric *gfp* expression in ASER. Circles indicate absent, ASEL alone, ASEL and ASER, and ASER alone, respectively.

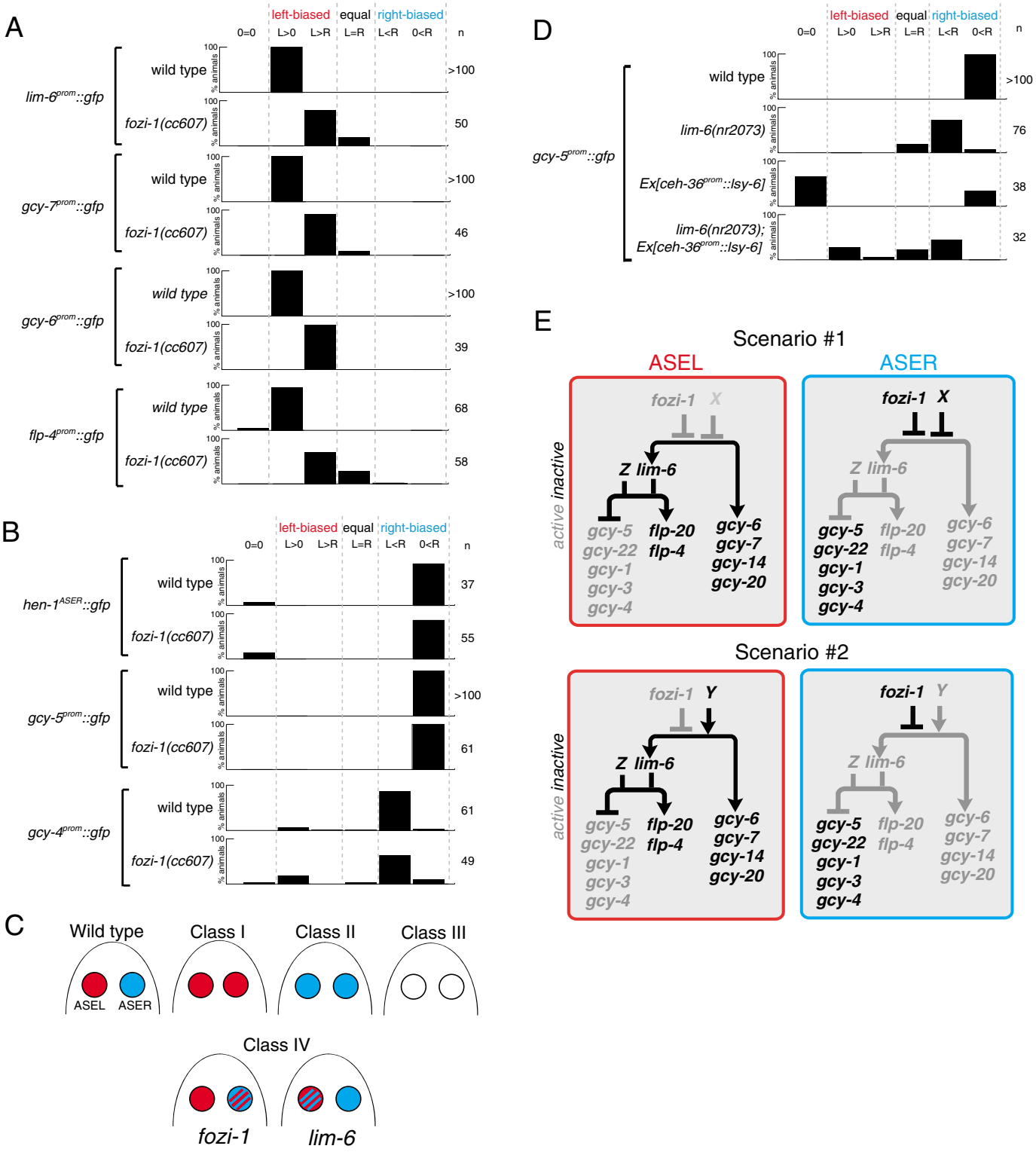


**Fig. 4. Analysis of ASEL and ASER fate in *fozi-1* and *lim-6* mutant animals.** (**A**) In *fozi-1(cc607)*-null mutant animals, ASEL-specific *lim-6*$^{prom}$*::gfp (otIs114)*, *flp-4*$^{prom}$*::gfp (otIs178), gcy-7* $^{prom}$*::gfp (otIs3)* and *gcy-6* $^{prom}$*::gfp (otIs162)* are de-repressed in ASER. '0=0' indicates no expression, 'L>0' indicates exclusive expression in ASEL, 'L>R' indicates expression in ASEL is stronger than in ASER, 'L=R' indicates equal expression in ASEL and ASER, 'L<R' indicates expression in ASER is stronger than in ASEL, and '0<R' indicates exclusive expression in ASER. (**B**) Analysis of ASER fate markers in *fozi-1(cc607)* null mutants. Reporter arrays used were *ntIs1 (gcy-5), otEx2409 (gcy-4)* and *otEx1274 (hen-1*$^{ASER}$*)*. (**C**) Summary of the *fozi-1* mutant phenotype and comparison with previously described ASE fate mutants. Blue circles indicate the ASEL-specific gene expression battery, red circles indicate the ASER-specific gene expression battery. (**D**) *lim-6* is not sufficient to repress ASER cell fate. (**E**) Summary of genetic interaction data. The incomplete expressivity of *fozi-1* and *lim-6* null alleles argues for the existence of parallel pathways (indicated by factor X, Y, Z). The two different scenarios make different predictions about the site of action of the parallel pathways. In scenario 1, it is active in ASER; in scenario 2, it is active in ASEL.

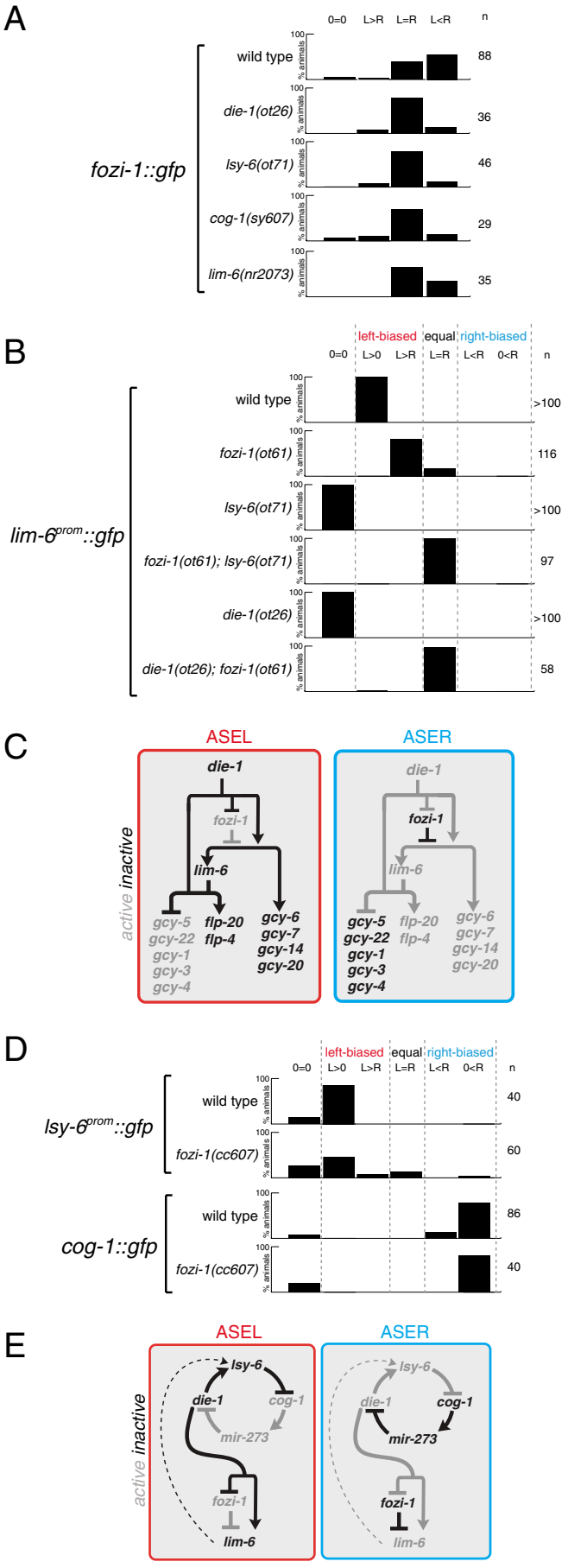


**Fig. 5. *fozi-1* acts downstream of the bi-stable feedback loop to control ASER differentiation.** (**A**) Asymmetric *fozi-1::gfp* expression (*otEx2192*; line #3 in Fig. 3C) is disrupted in *die-1(ot26), lsy-6(ot71)* and *cog-1(sy607)* null mutants animals, and partially affected in *lim-6*-null mutants. The 'L=R' category indicates equal expression in ASEL and ASER, including de-repression of *gfp* expression in ASEL (yielding strong *gfp* expression in both ASEL and ASER; *die-1* and *lsy-6* phenotype) and reduction of *gfp* expression in ASER (yielding equally low expression in ASEL and ASER; *cog-1* phenotype). (**B**) Removing *fozi-1* reverts the loss of *lim-6* expression *(otIs114)* observed in *lsy-6(ot71)* or *die-1(ot26)* mutant animals. (**C**) Summary of genetic interactions, pooling data from A and B, combined with the data from Fig. 4. The completely penetrant and expressive phenotype observed in *die-1* mutants argues that the pathways parallel to *fozi-1* and *lim-6* are under *die-1* control. The simplest explanation is that *die-1* itself acts in parallel to *fozi-1* and *lim-6* to control expression of target genes. (**D**) *fozi-1(cc607)* null mutant animals display weakly penetrant defects in *lsy-6* expression, assayed with *lsy-6*$^{prom}$*::gfp (otIs162)* and *cog-1* expression, assayed with *cog-1::gfp (syIs63)*. (**E**) Summary of the feedback data. The *lim-6*-dependent feedback to *lsy-6* (or *die-1*; for simplicity, the arrow only points to *lsy-6*), described in Johnston et al. (Johnston et al., 2005), is represented by a broken arrow to indicate that the effect is partially penetrant and only required to maintain the asymmetric expression of loop components.

## The Zn fingers but not the FH2 domain are essential for *fozi-1* function

All factors previously known to play roles in the lateral ASE cell fate decision are bona fide transcription factors or miRNAs. Therefore, we were surprised to have identified with *fozi-1* a gene that, on the one hand, contains conventional signatures of a transcription factor (Zn fingers and Q-rich domain), but on the other hand contains a FH2 domain, which has been characterized as a cytoplasmic actin-nucleation domain (Zigmond, 2004). This prompted us to learn more about the FH2 domain of FOZI-1 (henceforth termed FH2$^{FOZI-1}$).

Primary sequence comparison of FH2$^{FOZI-1}$ and other FH2 domains suggests that FH2$^{FOZI-1}$ is clearly related to FH2 domains (Fig. 6A). Secondary structure predictions of FH2$^{FOZI-1}$ also agree well with known FH2 domain structures. Homology modeling of FH2$^{FOZI-1}$ reveals that patterns of conservation in the hydrophobic cores of the lasso and post regions, two structural motifs involved in FH2 domain dimerization (Otomo et al., 2005; Xu et al., 2004), also allow a potential dimeric interaction of FH2$^{FOZI-1}$ domain (Fig. 6A,B). However, the similarity of FH2$^{FOZI-1}$ with other FH2 domains is poor in those regions that contact actin. In particular, two highly conserved amino acids, equivalent to Ile1431 and Lys1601 in the Bni1 FH2 domain, which have been shown to be essential for actin nucleation activity (Otomo et al., 2005; Xu et al., 2004), are altered in FH2$^{FOZI-1}$ (Fig. 6A). In addition, the linker between the lasso and knob regions, which is also important for actin nucleation function, is severely shortened in the FH2$^{FOZI-1}$, thereby likely reducing its flexibility. The FH2 domains of all other nematode FH2 domain proteins (six besides FOZI-1; http://smart.embl-heidelberg.de/) look like standard FH2 domains in terms of conservation of individual key residues and length of linker regions (data not shown). Taken together, our sequence analysis makes two predictions about FOZI-1, namely that FOZI-1 may still homodimerize via its FH2 domain but may have no role in controlling actin polymerization as it lacks actin-binding surfaces and as the ring structure made by FH2 domain dimers (Fig. 6B) may not be large enough to accommodate actin.

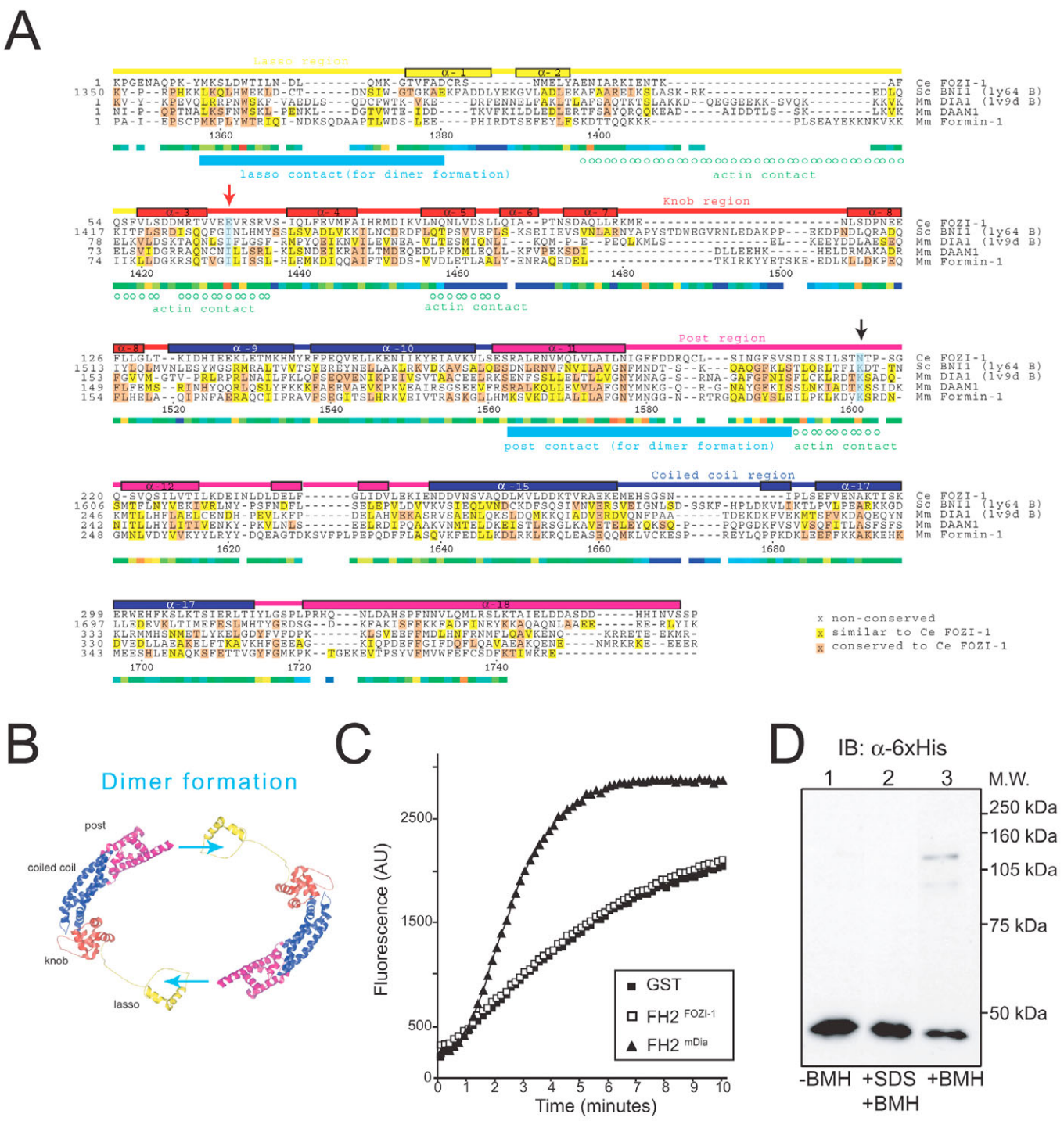


**Fig. 6. The FH2 domain of FOZI-1 is unusual and does not affect actin dynamics.** (**A**) Alignment of FH2$^{FOZI-1}$ with other FH2 domains, calculated with T-coffee version 2.03 (Notredame et al., 2000). FH2$^{FOZI-1}$ shows 9% to 20% sequence identity to other sequences in the alignment (49 FH2 domains from Pfam; only four shown here), which is in the range of sequence identities between the remaining FH2 domain sequences in the alignment. The sequence identities of FH2$^{FOZI-1}$ and FH2 domains of known structure, yeast FH2$^{Bni-1}$ [PDB-id:1y64; (Otomo et al., 2005)] and mouse FH2$^{Dia1}$ [PDB-id:1v9d; (Shimada et al., 2004)], are 16% and 14%, respectively. The profile-profile alignment program hmap (Tang et al., 2003) assigns a very good E-value (1.4e-26) for alignments between FH2$^{FOZI-1}$ and yeast FH2$^{Bni1}$. Secondary structure prediction for FH2$^{FOZI-1}$ also agrees well with the secondary structure found in the known structures (colored bar above alignment for FH2$^{Bni1}$). Neither Ile1431 nor Lys1601, which are crucial for the actin nucleation activity of the FH2 domains are conserved in FH2$^{FOZI-1}$ (red and black arrow). The colored bar at the bottom shows sequence conservation as calculated previously (Valdar, 2002) (red, high degree of conservation; blue, low degree of conservation). (**B**) Dimeric structure of the FH2 domain of yeast Bni1 (Otomo et al., 2005). (**C**) FH2$^{FOZI-1}$ does not stimulate actin polymerization. The FH2 domain of mouse Dia1 serves as a positive control. (**D**) FH2$^{FOZI-1}$ multimerizes. Isolated FH2$^{FOZI-1}$ (predicted to be 42 kDa) migrates as a single band (lane 1, –BMH). Treatment of FH2$^{FOZI-1}$ with the crosslinking reagent *Bis*-maleimidohexane (BMH) produces discrete slower migrating bands (lane 3, +BMH). The putative FH2 multimer is not present if the protein sample is denatured prior to crosslinking (lane 2, +SDS+BMH). FH2$^{FOZI-1}$ was detected by immunoblotting.

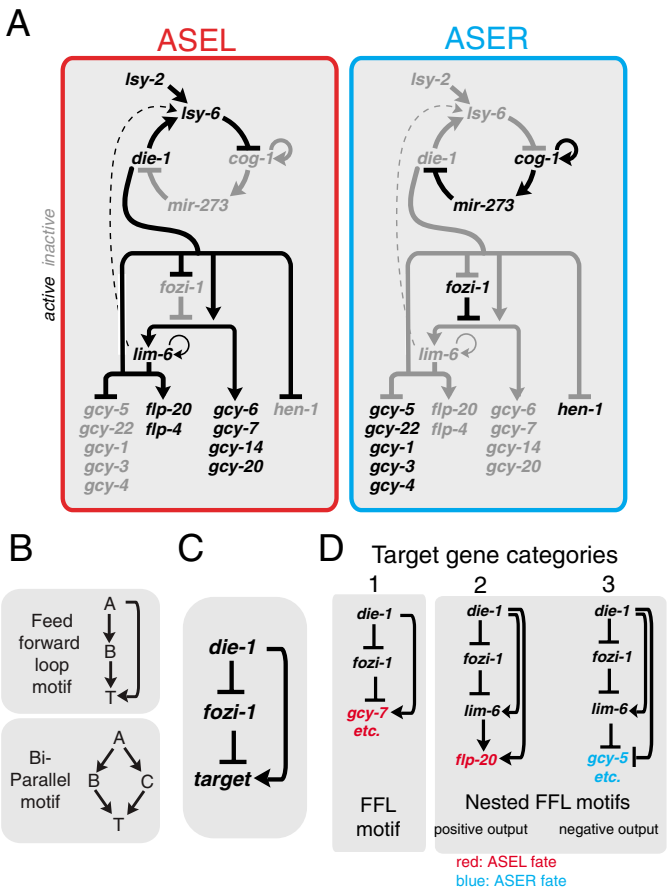


**Fig. 7. Summary of the gene regulatory architecture in the ASE neurons.** (**A**) Summary of regulatory interaction in ASEL and ASER. Broken line indicates partially penetrant feedback interaction (see Fig. 5E). See D for deconvolution of individual regulatory interactions. Several permissively acting factors, i.e. factors expressed in both ASEL and ASER (Chang et al., 2003) are not shown here for simplicity. Such factors could, for example, activate the ASER-expressed GCY genes in the absence of the ASEL repressors *die-1* and *lim-6*. (**B**) Network motifs. A FFL motif occurs when one gene (Gene A) controls a second gene (Gene B) and together these factors are required to regulate a target gene (Gene T). The addition of other factors (e.g. factor C) transforms the FFL motif to a 'bi-parallel motif' (Milo et al., 2002), which (analagous to FFL motifs) one could also envision to work as a persistence detector. (**C**) *die-1* and *fozi-1* may control target genes through a FFL motif. For a target to be activated, it requires both the presence of *die-1* and the absence of *fozi-1*. See D for identity of target genes. All arrows shown in this figure represent genetic interactions and do not necessarily imply direct physical interactions. Therefore, the identification of additional factors may alter network architecture. For example, *die-1* may not only repress *fozi-1* but also an additional factor, 'repressor Z', which together with *fozi-1* may repress ASEL-specific GCY genes. Such a repressor Z would transform the network motif from a FFL motif to a 'bi-parallel motif' (B). (**D**) Deconvoluted regulatory motifs extracted from A. Owing to their differential behavior upon loss of upstream regulators, ASE terminal differentiation genes can be placed into three distinct categories, all of which controlled by the basic FFL motif architecture shown in B. Target Gene Category 1: ASEL-specific expression of the GCY genes *gcy-6, gcy-7, gcy-14* and *gcy-20* does not require *lim-6,* but depends on the loop output regulator *die-1* and the downstream regulator *fozi-1*. As a complete elimination of *fozi-1* activity only results in partially expressive de-repression of the ASEL-specific GCY genes, an additional factor must be involved in repressing these GCY genes. This factor could be an unknown repressor that cooperates with *fozi-1* or, alternatively, the failure to completely activate ASEL-specific GCY genes in ASER may be due to the lack of an activator in ASER (Fig. 4E). The loop output regulator *die-1* is the best available candidate for this activator as *die-1* is predominantly expressed in ASEL and *die-1* mutation leads to a completely penetrant and expressive effect on ASEL-specific gene expression. As *die-1* also regulates *fozi-1*, the genetic interaction therefore may define a FFL motif. This motif is the most parsimonious illustration of the genetic observation that ASEL-specific genes depend on two different factors: the presence of *die-1* and the absence of *fozi-1*. Target Gene Categories 2 and 3: Regulation of genes in this category is distinguishable from control of Category 1 genes by the distinct role of the LIM homeobox gene *lim-6*. *die-1* represses *fozi-1* expression in ASEL; in the absence of *fozi-1*, *lim-6* is expressed. Together, *lim-6* and *die-1* (or a *die-1*-dependent pathway) activate ASEL-specific FLP genes and repress ASER-specific GCY genes in ASEL. This motif architecture is also a FFL motif, but now with an additional tier of regulation. Similar to the case of Category 1 target genes, the argument for this network architecture is revealed through the completely penetrant effect of disruption of the components of the feedback loop (including *die-1*) on all downstream genes (*lim-6, fozi-1* and terminal target genes), and the incompletely penetrant and expressive effect of *lim-6* on the terminal target genes. This incomplete penetrance and expressivity implies the need for another regulatory factor, for which *die-1* is at present the best candidate, given its completely penetrant and expressive effect on the terminal target genes. An additional potential feed-forward motif in the interaction of these factors is suggested by the incomplete penetrance of *fozi-1* on *lim-6* expression. As *lim-6* is affected by *die-1* in a completely penetrant manner, *lim-6* is controlled by a potential feed-forward loop, receiving inputs from *die-1* and *fozi-1*. This renders *lim-6* under the same control as the above mentioned ASEL-specific GCY genes, which are also controlled by a combination of *die-1* and *fozi-1*.

We tested these predictions using in vitro and in vivo assays. FH2 domains affect actin polymerization by either inducing polymerization of actin monomers or capping F-actin barbed ends (Kovar et al., 2003; Pruyne et al., 2002). We tested the ability of purified $FH2^{FOZI-1}$ to induce actin polymerization in vitro using the pyrene actin assay. In contrast to the control FH2 domain of the mouse FH2 protein Dia1, $FH2^{FOZI-1}$ is unable to induce actin polymerization (Fig. 6C). Similarly, $FH2^{FOZI-1}$ is unable to cap barbed ends (see Fig. S2A in the supplementary material) and does not bind actin filaments in sedimentation assays (data not shown). These experiments confirm the prediction that $FH2^{FOZI-1}$ has lost its role in regulating actin polymerization. The prediction that $FH2^{FOZI-1}$ still maintains its ability to dimerize is confirmed by our observation that purified $FH2^{FOZI-1}$ elutes from a Sephadex 200 gel filtration column as a single peak of ~100 kDa, consistent with the formation of a $FH2^{FOZI-1}$ dimer (see Fig. S2B in the supplementary material). In separate crosslinking experiments, the formation of $FH2^{FOZI-1}$ oligomers could also be detected (Fig. 6D).

We next tested the requirement of the FH2 domain and Zn fingers for *fozi-1* function in vivo. To this end, we made use of the rescue assay described above (Fig. 3A), in which a *gfp* tagged *fozi-1* cDNA is expressed under control of an ASER-specific promoter. Multiple transgenic lines were generated that express constructs in which individual domains of *fozi-1* were deleted. All constructs showed, as assessed by their *gfp* tag, comparable expression levels in the nucleus of ASER (data not shown). We found that deleting the Zn fingers completely eliminates rescuing ability of the *fozi-1* cDNA, demonstrating that the Zn fingers are essential for *fozi-1* function in

ASER (Fig. 3A). As FOZI-1 primarily localizes to the nucleus (Fig. 3B), requires its Zn fingers for function and is required for the repression of specific gene expression programs, we conclude that FOZI-1 probably is a transcriptional regulatory factor.

Examining the functional relevance of the FH2 domain, we found that deletion of the FH2 domain diminished but did not completely eliminate the ability of the *fozi-1::gfp* construct to rescue the *fozi-1* mutant phenotype (Fig. 3A). The FH2 domain of FOZI-1 therefore does not appear to be absolutely crucial for protein function, at least in the context of ASER differentiation.

In summary, FOZI-1 is unlikely to have a role in actin polymerization because: (1) there is no evidence for the existence of filamentous actin in the nucleus where FOZI-1 localizes; (2) detailed sequence analysis reveals that the FOZI-1 FH2 domain does not contain key features required for actin polymerization; (3) in vitro assays fail to reveal actin polymerization activity of the FOZI-1 FH2 domain; and (4) functional in vivo experiments indicate that the FH2 domain is not essential for gene function in the context of lateral ASE subclass specification. The only point that, at first sight, may argue for the importance of the FH2 domain is the *ot61* allele, which prematurely terminates the FH2 domain. However, this mutation does not only disrupt the FH2 domain, but de-stabilizes the complete protein, as evidenced by a complete loss of anti-FOZI-1 antibody staining in *ot61* mutant animals (J.L., unpublished).

## DISCUSSION

Few genes are known to function in a left/right asymmetric manner in bilaterally symmetric neuronal structures. Our genetic analysis establishes that *fozi-1* acts in a left/right asymmetric manner in the ASE gustatory neuron class to control the correct execution of a single neuron-specific, left/right asymmetric gene expression program (summarized in Fig. 7). Below, we first discuss specific structural features of the *fozi-1* gene and then describe how our analysis of *fozi-1* has revealed novel aspects of ASEL/R fate determination.

### The domain composition of FOZI-1 provides an example of domain rearrangement

The combination of FH2 and C2H2 Zn-finger domains in a single protein appears to be unique to the nematode lineage. The *fozi-1* gene probably originated by gene arrangement that joined two initially independent genes. What is the selective advantage of maintaining such a gene? The ancient function of the FH2 domain is to control actin polymerization given that FH2 domains from yeast to mammals harbor such an activity (Zigmond, 2004). However, our sequence and biochemical analysis suggests that the FH2 domain of FOZI-1 has lost this function. Nevertheless, the FH2 domain of FOZI-1 does harbor some function as its deletion compromises the ability to rescue the *fozi-1* mutant phenotype. Our analysis of the FH2 domain of FOZI-1 suggests that the domain has retained its ability to homodimerize, another ancient property of the domain that has been reported for all other characterized FH2 domain proteins. Transcription factors often dimerize, which increases their DNA-binding surface and enables cooperative DNA binding (Harrison, 1991). It is conceivable that the FOZI-1 FH2 domain serves the similar purpose of doubling the DNA contact surface of FOZI-1 through homodimerization. This may also explain why the FOZI-1 protein may still function, albeit only partially, upon deletion of the FH2 domain. In our in vivo rescue assays, transgenic array-induced overexpression of dimerization-defective FOZI-1 protein may increase the cellular FOZI-1 protein concentration enough to alleviate the need for dimerization-induced recruitment of proteins to DNA. Future identification of FOZI-1 DNA target sites and biochemical assays will test the validity of this hypothesis.

### *fozi-1* and *lim-6* mutants define a novel, 'mixed' ASE state

Previously, we have defined two states for ASEL/R gene expression profiles: hybrid and stable (Johnston et al., 2005). The hybrid state occurs in both ASEL and ASER during embryonic and early larval stages in which most ASE markers (including the ASEL-inducer *lsy-6* and the ASER-inducer *cog-1*) are expressed in both ASEL and ASER. Dependent on the activity of the bi-stable feedback loop, this hybrid state of gene expression subsequently becomes restricted to either the ASEL or ASER stable state. Genetic ablation of feedback loop components causes both ASE cells to take on the complete ASEL cell fate ('class I' mutants including *cog-1*) or the complete ASER cell fate ('class II' mutants including *lsy-6, die-1, lsy-2*).

*fozi-1* null mutant animals display an unusual phenotype. Rather than exhibiting a complete switch of cell fate in ASEL or ASER, *fozi-1* mutants display a 'mixed' fate phenotype in ASER. Whereas ASEL displays its ASEL-specific gene expression profile, ASER expresses ASEL terminal markers while maintaining expression of ASER terminal markers. In an almost mirror image of *fozi-1*-null mutant animals, *lim-6*-null mutant animals adopt an essentially normal ASER state in ASER but fail to repress specific ASER terminal markers in ASEL, again causing a 'mixed' state, this time in ASEL. Taken together, both *lim-6* (expressed in ASEL) and *fozi-1* (expressed in ASER) are regulatory intermediaries that transduce an output from the bi-stable feedback loop. These factors thereby enable the progression of differentiation states from a hybrid precursor state to a terminally differentiated end state.

### ASE subclass determination involves a complex regulatory architecture composed of several network motifs

Systematic analyses of gene regulatory networks in unicellular organisms have revealed that transcription factors interact in numerous combinations of simple network motifs (Lee et al., 2002; Shen-Orr et al., 2002). Here and in our previous work, we have extended the concept of defined network motifs to cell fate determination in the nervous system of metazoan organisms. We have shown (1) that a bi-stable feedback loop motif is a key decision point in the ASEL/R fate determination process (Johnston et al., 2005) and (2) that multiple distinct network motifs can be intertwined into a multi-tier regulatory architecture (this paper). The usefulness in considering these motifs in the context of ASEL/R cell fate determination lies in the well-defined properties of network motifs that can be mathematically modeled (Fig. 7B) and which provide clear predictions about the underlying logic of ASEL/R fate determination.

Specifically, the analysis of the *fozi-1* gene and its relationship with other regulatory network components suggests novel regulatory motifs that act in conjunction with the previously described bi-stable feedback loop. Emanating from the *die-1* Zn finger transcription factor, and including the *fozi-1* Zn finger factor, all these motifs appear to be variants of the feed-forward loop (FFL) network motif (Fig. 7B,C), a motif commonly found in transcription factor networks (Lee et al., 2002; Shen-Orr et al., 2002). A defining feature of FFL motifs is that they provide a persistence detector that measures whether a gene regulatory input persists long enough before target genes are activated (Fig. 7B) (Mangan and Alon, 2003; Mangan et al., 2003). In the cases described here, we infer the

existence of FFL network motifs based on the variable expressivity of null mutant phenotypes (see legend to Fig. 7D for detailed explanations). With the possible exception of *hen-1*, all left/right asymmetrically expressed genes may be regulated through FFL motifs. In each of these FFL motif configurations, *die-1* and *fozi-1* jointly regulate a target gene (Fig. 7C); expression of the target requires both the presence of *die-1* and the absence of *fozi-1*. The target gene is either a terminal differentiation marker (*gcy-7* etc.) or it is another regulatory factor, *lim-6*, which then activates FLP genes and represses ASER-specific GCY genes (Fig. 7D).

## Connecting gene regulatory network motifs

Apart from being the starting point for several presumptive feed-forward loops, the *die-1* Zn-finger transcription factor is the output regulator of a bi-stable, double-negative feedback loop, which contains additional transcription factors and miRNAs, and was the first network motif identified in ASE fate specification (Fig. 7A). *die-1* therefore represents a crucial 'node' in connecting the bi-stable feedback loop to the feed-forward loops described here. The theoretical behaviors of feedback and feed-forward motifs allow us to speculate on how the ASEL/R fate decision may occur. The bi-stable feedback loop may allow amplification of an initial, transient input into the system. Such an input could be an intrinsic, lineage-derived cue or an externally provided signal. After the reception of this input in a left/right asymmetric manner, the feedback loop may increase and/or stabilize *die-1* levels in ASEL. As the feed-forward loops that emanate from *die-1* may act as a persistence detector, target genes will become activated only once the feedback loop has ensured that *die-1* levels are persistently above a specific threshold level. The combined feedback and feed-forward regulatory motifs finely tune the system, amplifying a crucial input and assessing the stabilization and continuity of this amplification. We anticipate that the overall logic of the ASEL/R cell fate choice may apply to other cell fate decisions that have not yet been examined in extensive genetic detail.

We thank S. Mitani (Tokyo Women's Medical University School of Medicine) for the *tm563* allele, Y. Kohara for *fozi-1* EST clones, Q. Chen for expert injection assistance and P. Sengupta, U. Alon, C. Desplan and Hobert laboratory members for discussion and comments on the manuscript. This work was funded by an NSF predoctoral fellowship (R.J.J.) and by NIH R01 NS050266-01 (O.H.). B.H. and O.H. are Investigators of the Howard Hughes Medical Institute. J.C. is supported by a grant from CIHR.

### Supplementary material

Supplementary material for this article is available at http://dev.biologists.org/cgi/content/full/133/17/3317/DC1

### References

**Chang, S., Johnston, R. J., Jr and Hobert, O.** (2003). A transcriptional regulatory cascade that controls left/right asymmetry in chemosensory neurons of C. elegans. *Genes Dev.* **17**, 2123-2137.
**Chang, S., Johnston, R. J., Frokjaer-Jensen, C., Lockery, S. and Hobert, O.** (2004). MicroRNAs act sequentially and asymmetrically to control chemosensory laterality in the nematode. *Nature* **430**, 785-789.
**Copeland, J. W., Copeland, S. J. and Treisman, R.** (2004). Homo-oligomerization is essential for F-actin assembly by the formin family FH2 domain. *J. Biol. Chem.* **279**, 50250-50256.
**Davidson, E. H.** (2001). *Genomic Regulatory Systems*. San Diego: Academic Press.
**Fukushige, T., Hawkins, M. G. and McGhee, J. D.** (1998). The GATA-factor elt-2 is essential for formation of the Caenorhabditis elegans intestine. *Dev. Biol.* **198**, 286-302.
**Harrison, S. C.** (1991). A structural taxonomy of DNA-binding domains. *Nature* **353**, 715-719.
**Hobert, O.** (2002). PCR fusion-based approach to create reporter gene constructs for expression analysis in transgenic C. elegans. *Biotechniques* **32**, 728-730.
**Hobert, O., Tessmar, K. and Ruvkun, G.** (1999). The Caenorhabditis elegans lim-6 LIM homeobox gene regulates neurite outgrowth and function of particular GABAergic neurons. *Development* **126**, 1547-1562.
**Hodgkin, J. and Doniach, T.** (1997). Natural variation and copulatory plug formation in Caenorhabditis elegans. *Genetics* **146**, 149-164.
**Iuchi, S.** (2001). Three classes of C2H2 zinc finger proteins. *Cell. Mol. Life Sci.* **58**, 625-635.
**Johnston, R. J. and Hobert, O.** (2003). A microRNA controlling left/right neuronal asymmetry in Caenorhabditis elegans. *Nature* **426**, 845-849.
**Johnston, R. J., Jr and Hobert, O.** (2005). A novel C. elegans zinc finger transcription factor, lsy-2, required for the cell type-specific expression of the lsy-6 microRNA. *Development* **132**, 5451-5460.
**Johnston, R. J., Jr, Chang, S., Etchberger, J. F., Ortiz, C. O. and Hobert, O.** (2005). MicroRNAs acting in a double-negative feedback loop to control a neuronal cell fate decision. *Proc. Natl. Acad. Sci. USA* **102**, 12449-12454.
**Kovar, D. R., Kuhn, J. R., Tichy, A. L. and Pollard, T. D.** (2003). The fission yeast cytokinesis formin Cdc12p is a barbed end actin filament capping protein gated by profilin. *J. Cell Biol.* **161**, 875-887.
**Lee, T. I., Rinaldi, N. J., Robert, F., Odom, D. T., Bar-Joseph, Z., Gerber, G. K., Hannett, N. M., Harbison, C. T., Thompson, C. M., Simon, I. et al.** (2002). Transcriptional regulatory networks in Saccharomyces cerevisiae. *Science* **298**, 799-804.
**Mangan, S. and Alon, U.** (2003). Structure and function of the feed-forward loop network motif. *Proc. Natl. Acad. Sci. USA* **100**, 11980-11985.
**Mangan, S., Zaslaver, A. and Alon, U.** (2003). The coherent feedforward loop serves as a sign-sensitive delay element in transcription networks. *J. Mol. Biol.* **334**, 197-204.
**Milo, R., Shen-Orr, S., Itzkovitz, S., Kashtan, N., Chklovskii, D. and Alon, U.** (2002). Network motifs: simple building blocks of complex networks. *Science* **298**, 824-827.
**Notredame, C., Higgins, D. G. and Heringa, J.** (2000). T-Coffee: A novel method for fast and accurate multiple sequence alignment. *J. Mol. Biol.* **302**, 205-217.
**Ortiz, C. O., Etchberger, J. F., Posy, S. L., Frøkjær-Jensen, C., Lockery, S., Honig, B. and Hobert, O.** (2006). Searching for neuronal left/right asymmetry: Genome wide analysis of nematode receptor-type guanylyl cyclases. *Genetics* **173**, 131-149.
**Otomo, T., Tomchick, D. R., Otomo, C., Panchal, S. C., Machius, M. and Rosen, M. K.** (2005). Structural basis of actin filament nucleation and processive capping by a formin homology 2 domain. *Nature* **433**, 488-494.
**Pierce-Shimomura, J. T., Faumont, S., Gaston, M. R., Pearson, B. J. and Lockery, S. R.** (2001). The homeobox gene lim-6 is required for distinct chemosensory representations in C. elegans. *Nature* **410**, 694-698.
**Pruyne, D., Evangelista, M., Yang, C., Bi, E., Zigmond, S., Bretscher, A. and Boone, C.** (2002). Role of formins in actin assembly: nucleation and barbed-end association. *Science* **297**, 612-615.
**Shen-Orr, S. S., Milo, R., Mangan, S. and Alon, U.** (2002). Network motifs in the transcriptional regulation network of Escherichia coli. *Nat. Genet.* **31**, 64-68.
**Shimada, A., Nyitrai, M., Vetter, I. R., Kuhlmann, D., Bugyi, B., Narumiya, S., Geeves, M. A. and Wittinghofer, A.** (2004). The core FH2 domain of diaphanous-related formins is an elongated actin binding protein that inhibits polymerization. *Mol. Cell* **13**, 511-522.
**Simmer, F., Tijsterman, M., Parrish, S., Koushika, S., Nonet, M., Fire, A., Ahringer, J. and Plasterk, R.** (2002). Loss of the putative RNA-directed RNA polymerase RRF-3 makes C. elegans hypersensitive to RNAi. *Curr. Biol.* **12**, 1317.
**Tang, C. L., Xie, L., Koh, I. Y., Posy, S., Alexov, E. and Honig, B.** (2003). On the role of structural information in remote homology detection and sequence alignment: new methods using hybrid sequence profiles. *J. Mol. Biol.* **334**, 1043-1062.
**Titz, B., Thomas, S., Rajagopala, S. V., Chiba, T., Ito, T. and Uetz, P.** (2006). Transcriptional activators in yeast. *Nucleic Acids Res.* **34**, 955-967.
**Valdar, W. S.** (2002). Scoring residue conservation. *Proteins* **48**, 227-241.
**White, J. G., Southgate, E., Thomson, J. N. and Brenner, S.** (1986). The structure of the nervous system of the nematode *Caenorhabditis elegans*. *Philos. Trans. R. Soc. Lond. B Biol. Sci.* **314**, 1-340.
**Xu, Y., Moseley, J. B., Sagot, I., Poy, F., Pellman, D., Goode, B. L. and Eck, M. J.** (2004). Crystal structures of a Formin Homology-2 domain reveal a tethered dimer architecture. *Cell* **116**, 711-723.
**Yu, S., Avery, L., Baude, E. and Garbers, D. L.** (1997). Guanylyl cyclase expression in specific sensory neurons: a new family of chemosensory receptors. *Proc. Natl. Acad. Sci. USA* **94**, 3384-3387.
**Zigmond, S. H.** (2004). Formin-induced nucleation of actin filaments. *Curr. Opin. Cell Biol.* **16**, 99-105.